LASER INTERFEROMETER GRAVITATIONAL WAVE OBSERVATORY
- LIGO -
CALIFORNIA INSTITUTE OF TECHNOLOGY
MASSACHUSETTS INSTITUTE OF TECHNOLOGY

Technical Note	**LIGO-T11XXXXX–vX**	2017/06/30

Squeezing Quantum Noise with Waveguides
Interim Report 2 for SURF 2017

Dhruva Ganapathy

California Institute of Technology
LIGO Project, MS 18-34
Pasadena, CA 91125
Phone (626) 395-2129
Fax (626) 304-9834
E-mail: info@ligo.caltech.edu

Massachusetts Institute of Technology
LIGO Project, Room NW22-295
Cambridge, MA 02139
Phone (617) 253-4824
Fax (617) 253-7014
E-mail: info@ligo.mit.edu

LIGO Hanford Observatory
Route 10, Mile Marker 2
Richland, WA 99352
Phone (509) 372-8106
Fax (509) 372-8137
E-mail: info@ligo.caltech.edu

LIGO Livingston Observatory
19100 LIGO Lane
Livingston, LA 70754
Phone (225) 686-3100
Fax (225) 686-7189
E-mail: info@ligo.caltech.edu

http://www.ligo.caltech.edu/

1 Introduction

1.1 LIGO

The LIGO gravitational wave detectors are specialized versions of a Michelson interferometer with 4 km long arms with Fabry Perot cavities. Its peak design sensitivity is 3.5×10^{-24} in the 100 Hz band[1] , When it reaches design sensitivity it will be quantum noise limited over much of the detection band[2]. The Advanced LIGO (aLIGO) detectors came online in September 2015, after a major upgrade targeting a factor of 10 sensitivity improvement over initial detectors. The two test masses are placed 4 km apart and form an optical resonator with a gain of 300. The suspension system provides high isolation above the resonance frequencies which range from 0.4 to 13 Hz.

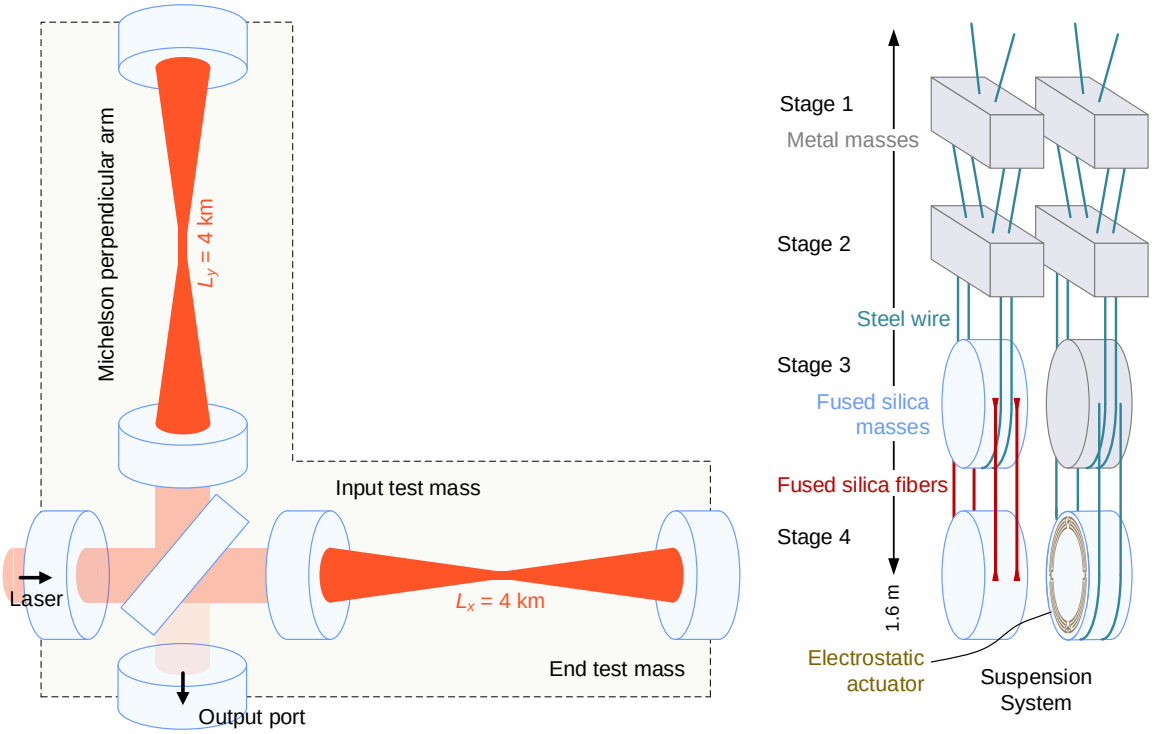

Figure 1: aLIGO

1.2 Squeezed Light

In an upgrade to aLIGO [3], work is underway to install a parametric oscillator squeezed vacuum light source to reduce quantum shot noise which limits the sensitivity of gravitational wave detector. This noise arises due to vacuum fluctuations which occur due to Heisenbergs uncertainty principle which states that $\Delta X \Delta Y > 1$ where X and Y are uncertainty in the quadratures associated with the photon field and are given by the expressions :

$$X = (a + a^\dagger)$$

$$Y = -i(a - a^\dagger)$$

Where a and $a\dagger$ are bosonic annihilation and creation operators respectively.

Vacuum is the ground state of a photon field and it is a coherent state. Coherent states are minimum uncertainty states where $\Delta X = \Delta Y = 1$. These uncertainties give rise to vacuum fluctuations which enter the unused port of the interferometer of the gravitational wave detector. The noise arising from these uncertainties can be understood by Figure 2.

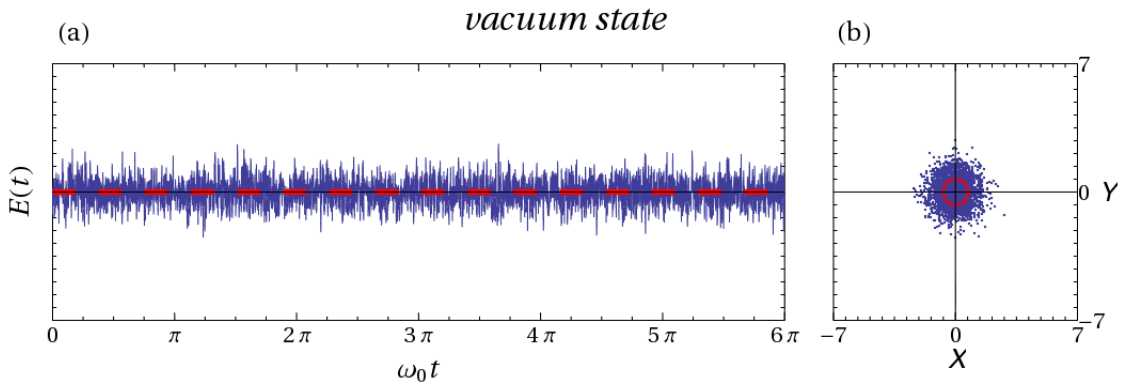

Figure 2: Electric Field in Coherent Vacuum

Squeezed states are also minimum uncertainty states. Here, the noise in one quadrature is greater than that in the other. Replacing the vacuum fluctuations with squeezed states in GW interferometers can reduce the quantum noise measured by the detector.

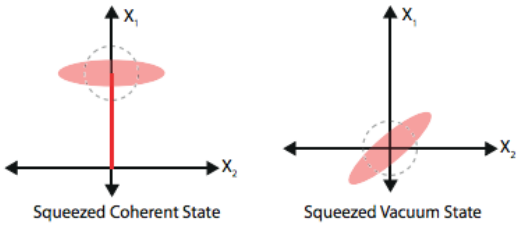

Figure 3: Quadrature Diagrams for Squeezed Light

Squeezing has already been implemented twice in working GW detectors [4],[5] and is a proven technology for enhancing signal to shot noise sensitive by 3.5 dB and 2.1 dB for the GEO600 and Enhanced LIGO detectors respectively. Squeezing injection is planned as a permanent feature in the next round of intermediate upgrades. More details about squeezed light can be found in [6].

2 Project

2.1 Objective

This project will investigate the spatial mode profiles emitted from a wave-guide type non-linear squeezer devices, examine the optimum index profile, pumping field shape and out

coupling scheme for generating high quantum efficiency modes for use in free space, and investigate how imperfections in the mode shapes affect the level of squeezing improvement ultimately achievable in a GW detector.

2.2 Approach

2.2.1 Setup

The project setup is shown in Figure 4. The Innolight Diabolo laser is a source of 532 nm and 1064 nm photons for the experiment. It consists of a 1.5 W Nd:YAG NPRO laser (pumped with two banks of diode lasers) with most of this light tapped off to an SHG unit for conversion to 532 nm. The green 532nm photons undergo Spontaneous Parametric Down-Conversion in a compact non-linear waveguide. Single mode squeezing is obtained when the SPDC is degenerate, i.e, the produced photons are indistinguishable.

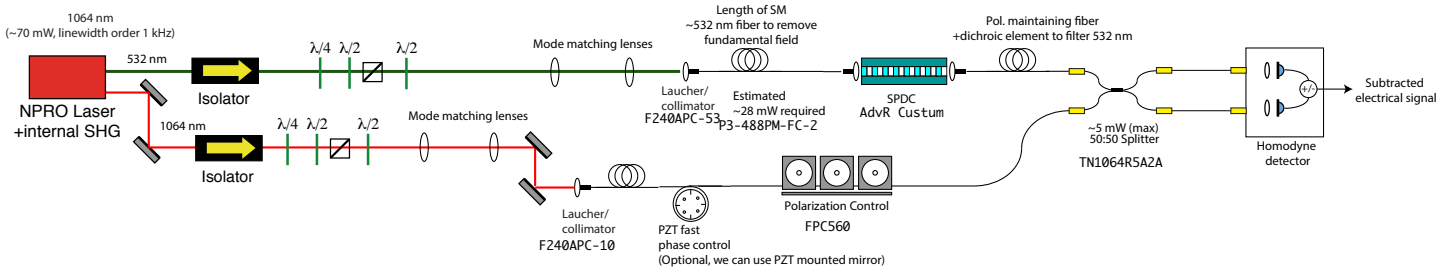

Figure 4: Proposed Setup for Waveguide Experiment

2.2.2 Mode Matching and Beam Propagation

One part of this project would involve modelling mode-matching between the wave-guide and the optical cavity of the resonator. For the optical waveguide, we will be considering a rectangular core waveguide with a step index.

To find the mode shapes of this waveguide, we can assume a separable solution of the scalar wave equation in rectangular coordinates.

$$\frac{\partial^2 \psi}{\partial x^2} + \frac{\partial^2 \psi}{\partial y^2} + [k_o^2 n^2(x,y) - \beta^2] = 0 \tag{1}$$

where β is the propagation constant and k_o is the free space wave number.

The solution obtained for this equation is given by

$$\psi = \begin{cases} A\cos\mu_1\xi\cos\mu_2\eta & \text{if}|\xi| \le 1, |\eta| \le 1 \\ \dfrac{A\cos\mu_2}{\exp[-(V_2^2-\mu_2^2)]^{\frac{1}{2}}}\cos\mu_1\xi\exp[-(V_2^2-\mu_2^2)\eta]^{\frac{1}{2}} & \text{if } |\xi| \ge 1, |\eta| \le 1 \\ \dfrac{A\cos\mu_1}{\exp[-(V_1^2-\mu_1^2)]^{\frac{1}{2}}}\cos\mu_2\eta\exp[-(V_1^2-\mu_1^2)\xi]^{\frac{1}{2}} & \text{if } |\xi| \le 1, |\eta| \ge 1 \\ \dfrac{\exp[-(V_2^2-\mu_2^2)\eta]^{\frac{1}{2}}\exp[-(V_1^2-\mu_1^2)\xi]^{\frac{1}{2}}}{\exp[-(V_1^2-\mu_1^2)]^{\frac{1}{2}}\exp[-(V_2^2-\mu_2^2)]^{\frac{1}{2}}} & \text{if } |\xi| \ge 1, |\eta| \ge 1 \end{cases} \quad (2)$$

where

$$\xi = (2x/a), \quad \eta = (2y/b), \quad V_1 = k_o\frac{a}{2}(n_1^2-n_2^2)^{\frac{1}{2}}, \quad V_2 = k_o\frac{b}{2}(n_1^2-n_2^2)^{\frac{1}{2}}$$

$$\mu_1 = \frac{a}{2}(k_o^2n_1^2-\beta^2)^{\frac{1}{2}}, \quad \mu_2 = \frac{b}{2}(k_o^2n_1^2-\beta^2)^{\frac{1}{2}}$$

A detailed solution of this equation is described in [7]. The effect of imperfections in the step index can be modelled by methods such as perturbation and scalar variational methods.

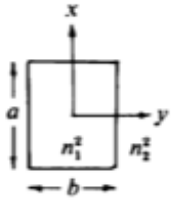

Figure 5: Rectangular Core Waveguide

The normal modes supported by the optical cavity, or any complex paraxial optical system, are higher order Gaussian or Hermite-Gaussian modes. These modes are given by

$$\tilde{u}_n = \tilde{\alpha}_n\tilde{v}^nH_n(\frac{\sqrt{2}x}{\tilde{v}})\exp(-\frac{r^2}{w(z)^2})\exp(-i\frac{kr^2}{2R(z)})\exp(-i(kz-\psi(z)))$$

where H_n is the n^{th} order Hermite polynomial, and $\psi(z)$ is the Gouy Phase of the beam

2.3 Beam Propagation

2.3.1 ABCD Propagation

When a Gaussian beam propagates in free space, it remains Gaussian, while its spot size and radius of curvature vary according to the wave equation. Now the beam at a point can be characterised by the following quantity.

$$q = z + iz_r$$

where z_r is the Rayleigh range of the beam, and z is the distance of the point from the waist.

The inverse of q contains a information about the spot size and radius of curvature of the beam. Substituting $w(z)$ and $R(z)$, we get

$$\frac{1}{q} = \frac{1}{R(z)} - \frac{i\lambda}{\pi w^2(z)}$$

If we specify the initial value of q, then we can use the ABCD propagation matrices for determining the final value of q[8].

$$q_2 = \frac{Aq_1 + B}{Cq_1 + D}$$

The matrices that we use in this project are -

$$\begin{pmatrix} A & B \\ C & D \end{pmatrix} = \begin{pmatrix} 1 & d \\ 0 & 1 \end{pmatrix}$$

for free space propagation through distance d and

$$\begin{pmatrix} A & B \\ C & D \end{pmatrix} = \begin{pmatrix} 1 & 0 \\ -\frac{1}{f} & 1 \end{pmatrix}$$

for propagation through lens with focal length f.

2.3.2 FFT Propagation

While ABCD propagation is a convinient method and can be used as a reference for other propagation methods, it is only applicable to the mode shapes of Gaussian beams. The mode outside the waveguide will not be a Gaussian and we will need other methods to find its mode shape after propagation in free space. One such method that we have implemented is FFT propagation of the beam[9].

According to the Huygens integral,

$$E(x, y, z) = \frac{i}{\Delta z \lambda} \iint E_0(x, y, z_0) K(x - u, y - v, \Delta z) du dv$$

which can be seen as a convolution of the source field E_0 at z_0 and the paraxial diffraction kernel.

In the fourier space, this is just the product of the Fourier Transform of the field and the FT of the diffraction kernel which is given by

$$\tilde{K}(p, q, \Delta z) = \exp\left(-i \frac{\Delta z (p^2 + q^2)}{2k}\right)$$

.

The final mode can be found out by taking an inverse fourier transform of the product. In our code we have used the fft2, and ifft2 functions of MATLAB to implement this routine.

2.3.3 Detecting Squeezed States

Balanced homodyne is an interference setup that is used for quadrature measurements. The field that is to be measured is overlapped with a local oscillator on a symmetric beam splitter, whose outputs impinge of two photodiodes, whose photocurrents are electronically subtracted. The phase of the local oscillator beam is controlled via a piezzo-electric transducer. The subtracted photocurrent is analysed using time domain and frequency domain approaches as described in [6].

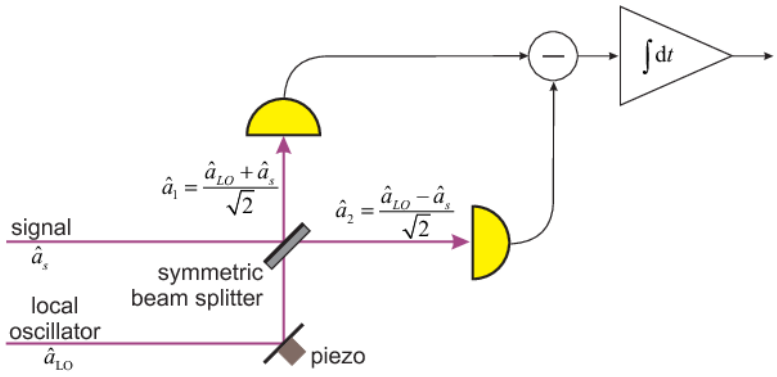

Figure 6: Balanced Homodyning Scheme

In order to properly detect squeezed states, we also need to take into account the noise that affects the homodyning process. The source of this noise includes electronic noise such as flicker in resistors and dark noise of photodiode, and optical noise due to scattering loss, photodiode inhomogeneity and parasitic interferences. These sources and methods to reduce them have been described in [10].

2.4 Progress

2.4.1 Setup

Figure 7 describes the internal working of the Diabolo laser and shows the two different outputs. Figure 8 shows the current state of the experiment .

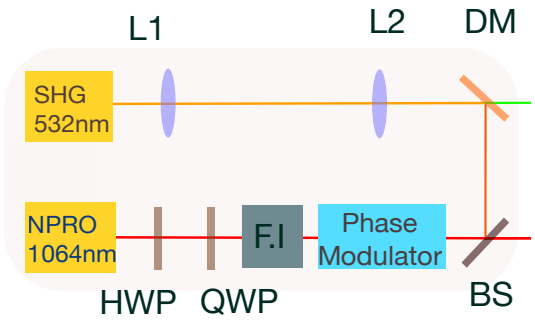

Figure 7: Innolight Diabolo

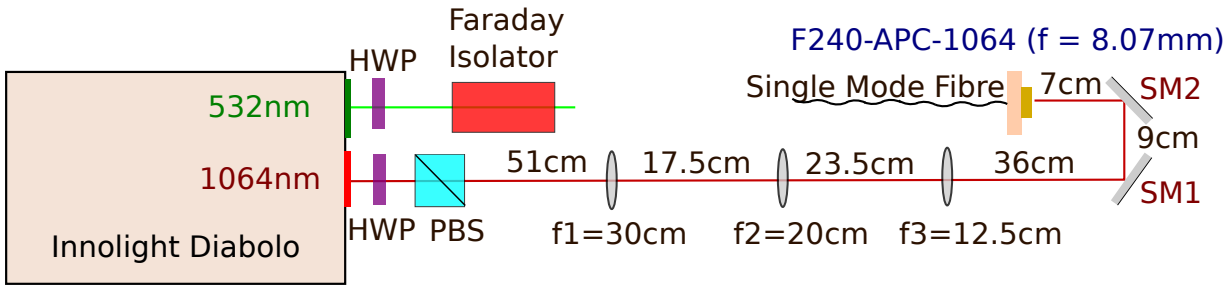

Figure 8: Current State of Experiment

In 7, L1 and L2 are mode matching lenses, DM is a dichroic mirror which reflects 1064nm and transmits 532nm, BS is a 50% beamsplitter, and F.I is a Faraday Isolator. In figure 8, F240-APC-1064 is the collimation package for transmitting the laser from free space into the 1064nm Single mode fibre. The light from this fibre will first be used for characterisation of the waveguide through SHG phase matching curves.

2.4.2 Beam Profiling

The following are the results of profiling the 1064nm and 532 nm beams from the Innolight Diabolo laser.

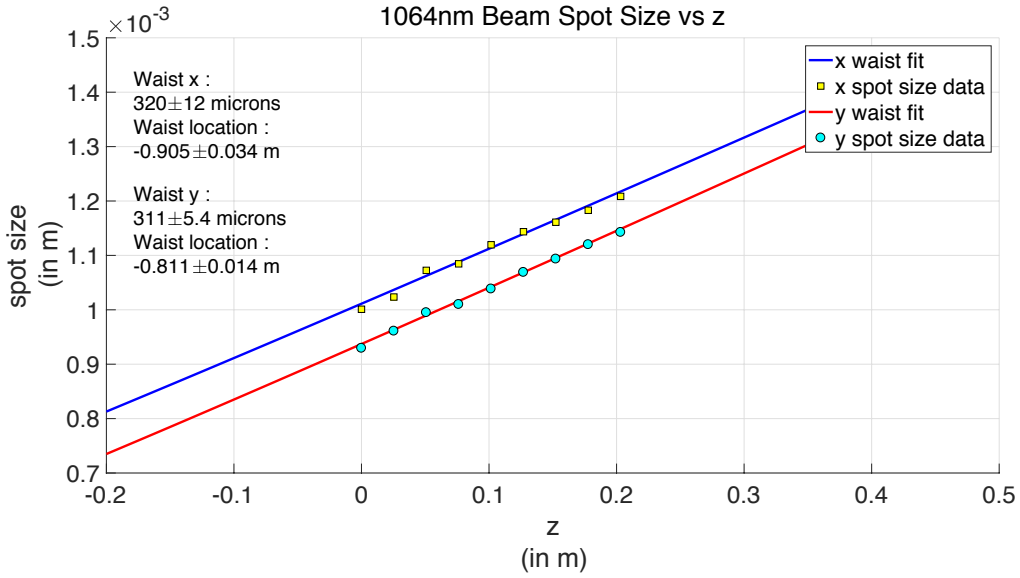

Figure 9: Beam Profiling the 1064nm laser

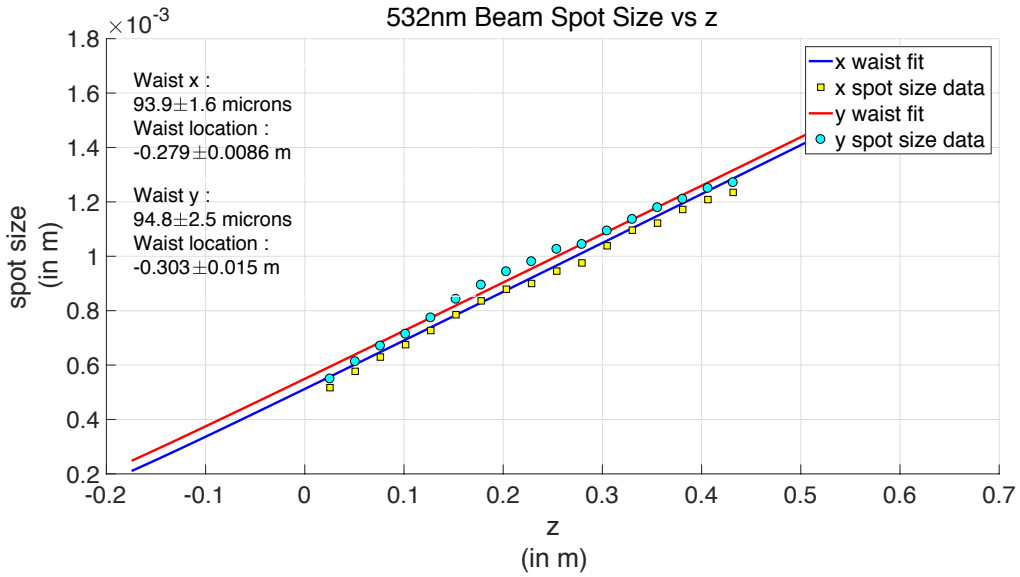

Figure 10: Beam Profiling the 532nm laser

2.4.3 Mode Matching of 1064nm Beam

The 1064nm beam has to be collimated in free space and then focused into a single mode fibre with the help of the collimation package F240-APC-1064. This package has a collimated beam size of 880 microns and a beam divergence of 0.04 degrees. In order to achieve efficient coupling, we need to make sure that the beam waist of the beam that we are focusing into the fibre is close to the above size. Working at a 3 lens solution, we first add a lens (f=30cm) in the beam path at z = 105cm, and profile the beam again to find a more accurate value for the beam waist size and location.

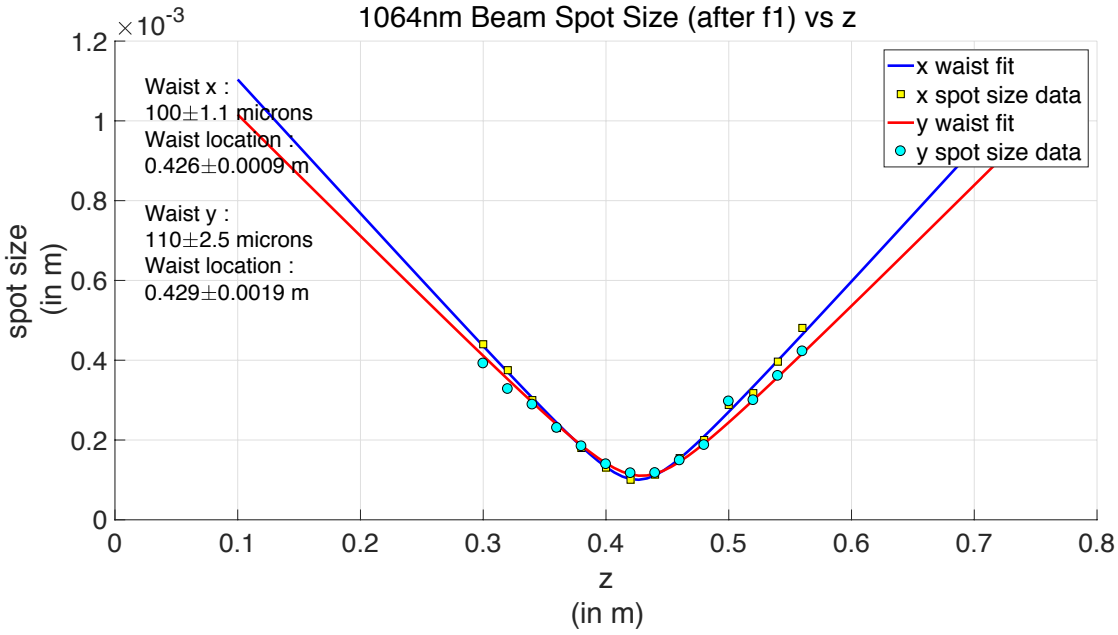

Figure 11: 1064nm beam profile after the first lens. z=0 is the location of the lens

Trial and error gives us a modified value of the initial beam waist to be 275 microns and location as -80cm from the arbitrarily chosen z=0 point. Over here, for the sake of simplicity, we will assume that the x and y waists of the beam are approximately equal as the amount of squeezing does not depend on the coupling efficiency at this interface and we just need significant power in the fibre.

Using these modified values, we calculated a mode-matching solution with 3 lenses using ABCD propagation.

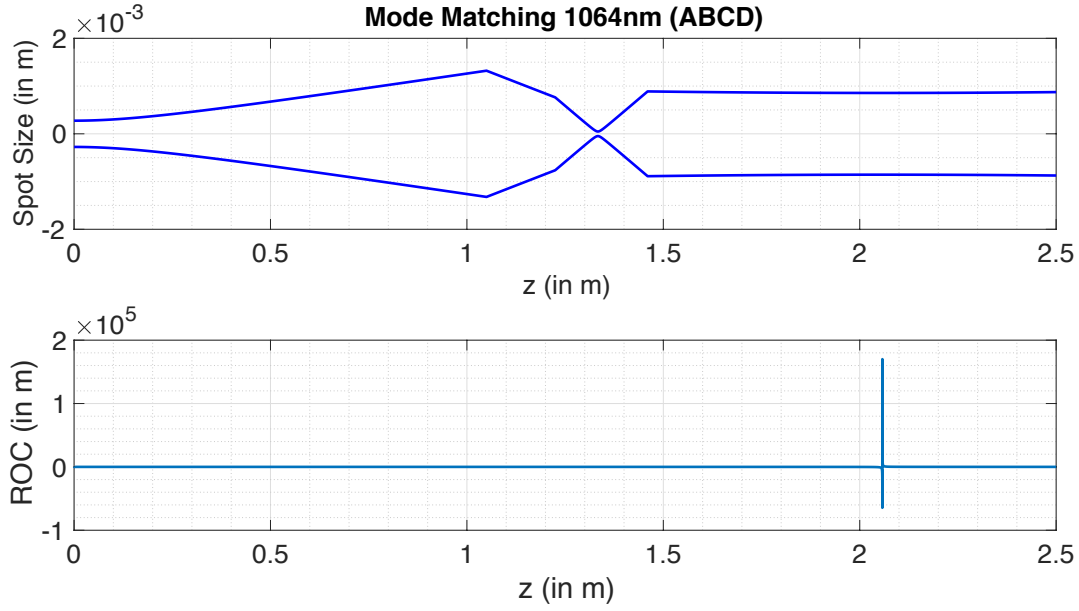

Figure 12: Mode Matching Solution for 1064nm (Waist at z=0)

The 3 lens solution Figure 12 is as follows -
f = 30cm at z = 105cm
f = 20cm at z = 122.5cm
f = 12.5cm at z = 146cm

The obtained beam waist of the collimated beam is 855.9 microns that is very close to the required 880 microns. Neglecting beam divergence of the collimator, we obtain the theoretical coupling efficiency to be 99.8%. The actual mode matching that is possible to achieve is lower than this because there are many factors to account for like defects in the lens, or astigmatism of the beam and the errors in lens locations.

In order to confirm this solution, we profile the beam after placing the second lens (f=20cm) at z=122.5cm.

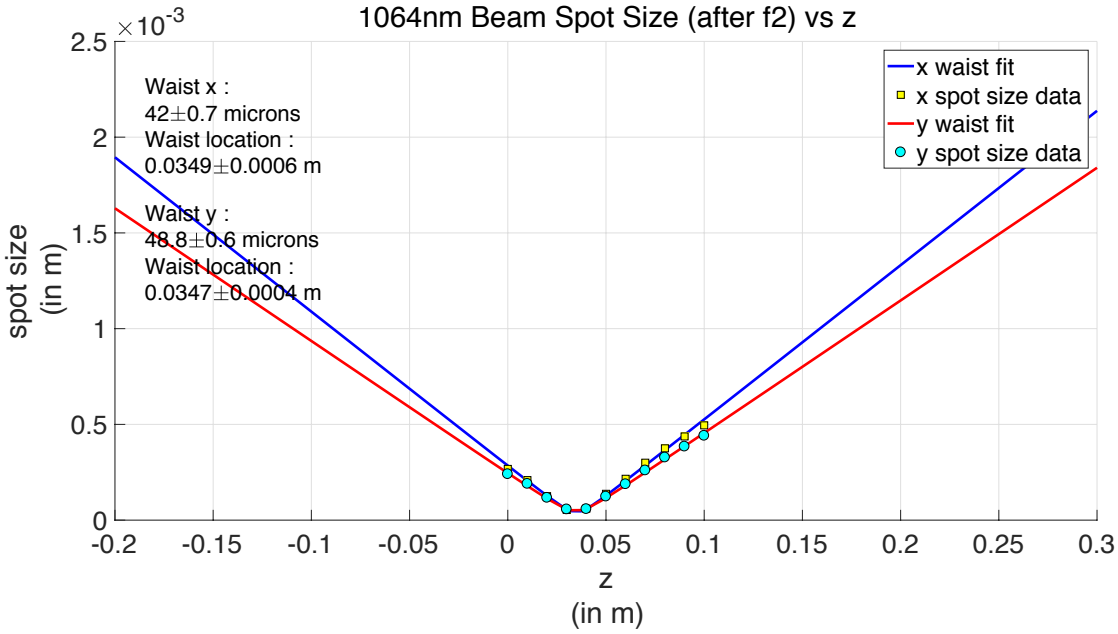

Figure 13: 1064nm beam profile after the second lens. z=0 is the location of the lens

The size and location of the second waist corresponds to that obtained by the ABCD simulation of the solution.

Note - As of now, efficient coupling has not been achieved (maximum 10%) in the experiment, due to issues with the fibre and alignment. We will attempt to use back-coupling to get a more accurate alignment.

2.4.4 Mode Matching of 532nm Beam

Just like the 1064nm beam, we also need to mode match the 532nm beam into a fibre using F240APC-532 collimation package. The required beam spot size for this is 740 microns. The solution that we obtain using ABCD propagation is as follows -

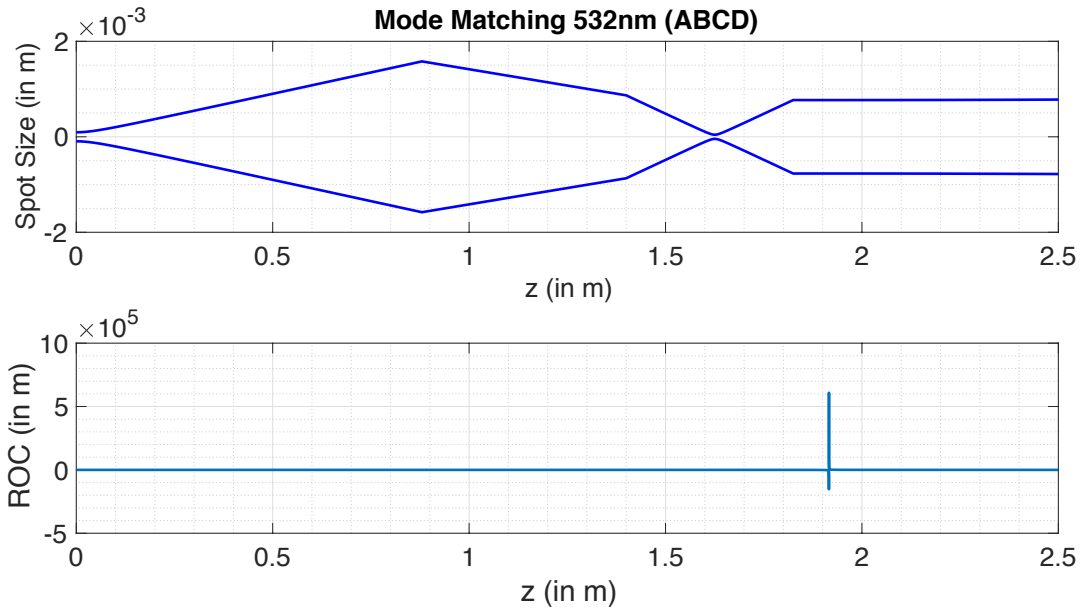

Figure 14: Mode Matching Solution for 532nm. (Waist at z=0)

The 3 lens solution Figure 14 is as follows -
f = 50cm at z = 88cm
f = 35cm at z = 140cm
f = 20cm at z = 182.5cm

According to this solution, the final beam waist is 720.4 microns which theoretically gives a coupling efficiency of 99.8%. The obtained coupling will be lower than this due to earlier mentioned reasons.

We will follow the same procedure as we did in the case of the 1064 nm beam to obtain a more accurate solution for the mode matching, i.e. we will add the first lens and then profile the beam to adjust the values of beam waist and location, and then profile after the second lens to confirm the solution

2.5 Waveguide Mode Shape

The Rubidium Infused PPKTP waveguide is a 7 micron x 7 micron square waveguide. As described in Section 2.2.2, the solution is a separable in x and y. To solve for the exact values of μ_1 and μ_2, we must solve the following transcendental equation.

$$\mu \tan \mu = \sqrt{V^2 - \mu^2}$$

As the waveguide is symmetric, $\mu_1 = \mu_2 = \mu$ and $V_1 = V_2 = V$.

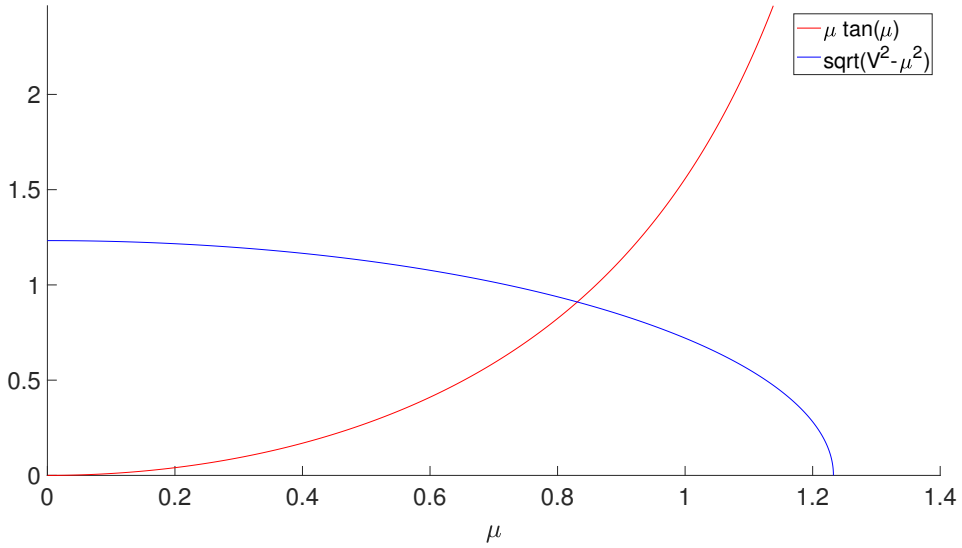

Figure 15: Transcendental equation for μ

The value obtained for μ is 0.8325. The mode shape obtained is shown in Figure 16

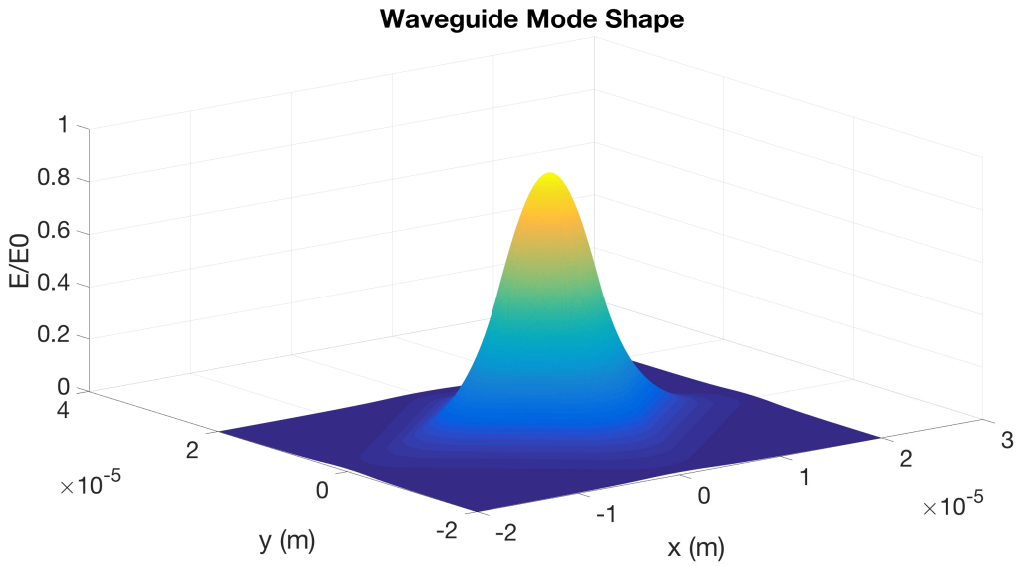

Figure 16: Waveguide Mode Shape

2.6 To Do

2.6.1 Characterisation of Waveguide

The non-linear waveguide has been set up along with temperature control. Once light is coupled efficiently into the 1064nm fibre, we will plot phase matching curves for SHG (Second Harmonic Generation) the waveguide by varying its temperature.

2.6.2 Calculation of Squeezing Losses

The waveguide has been butt-coupled to a fibre. The loss in squeezing can be calculating the overlap integral between the waveguide mode shape and the fibre mode.

2.6.3 Homodyne Detection

Design and assemble a transimpendance circuit for the photodetectors that will be used in the homodyning process. For stability, a capacitor must be placed in parallel with the resistor R_f. Two of these circuits must be constructed and subtracted using another op-amp circuit in order to obtain the homodyne signal.

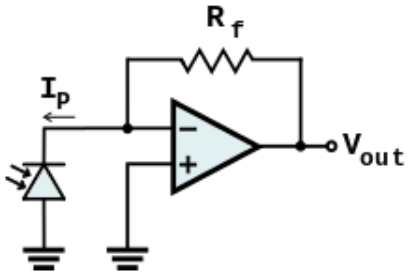

Figure 17: Simple Transimpedance Circuit

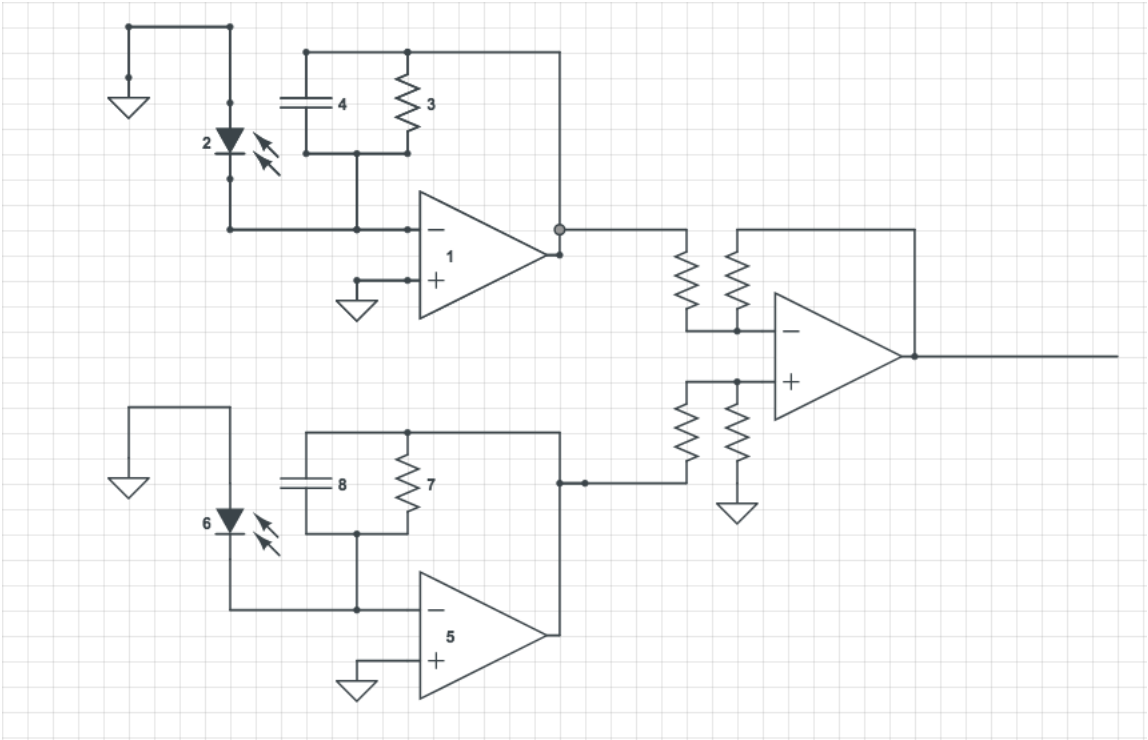

Figure 18: Homodyne Circuit

3 Appendix

3.1 Beam Profiling

The properties of the Gaussian beam depend only on the size of the waist w_0 and the wavelength λ. It is therefore possible to fully characterize a Gaussian beam by determining the size and location of the beam waist. To determine these quantities, we make a series of 'knife edge' measurements to determine the spot size on different axial locations.

We record the total power in the beam as a knife edge is translated through the beam using a calibrated translation stage. This gives us the integral of the power from $-\infty$ to the knife edge location.

In one direction this power is given by

$$P(y) = \frac{P_{total}}{2}(1 - \mathrm{erf}(\frac{\sqrt{2}(y - y_0)}{w_y}))$$

Fitting the obtained power to the above function gives us the spot size at the location of profiling

The obtained spot sizes are fit to the function

$$w(z) = w_0\sqrt{1 + (\frac{z - z_0}{z_r})^2}$$

where $z_r = \frac{\pi w_0^2}{\lambda}$

in order to find the beam waist size and location.

Following are a few results from profiling a He-Ne laser, in preparation for profiling the Diabolo laser.

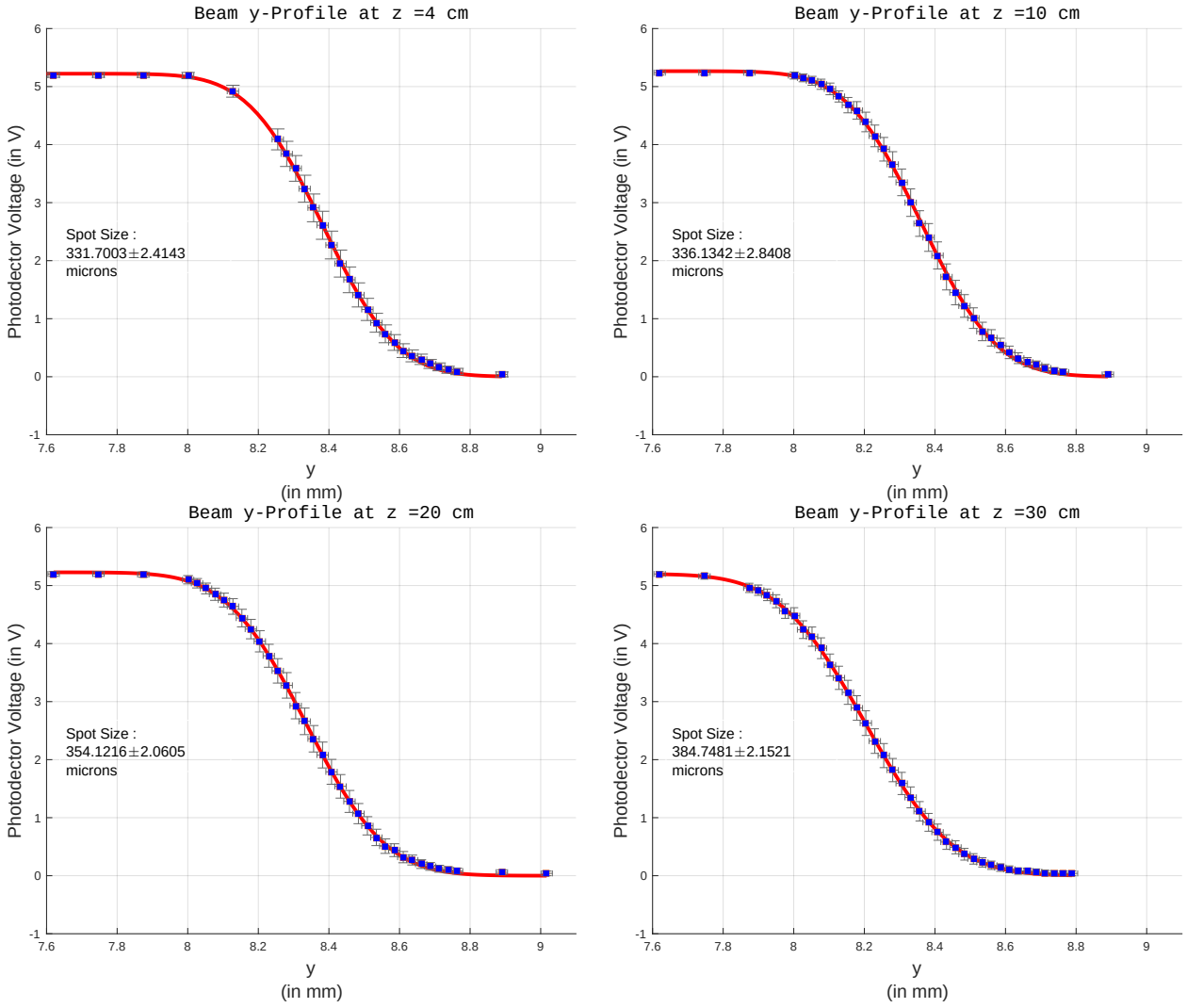

Figure 19: Beam Profiling Results

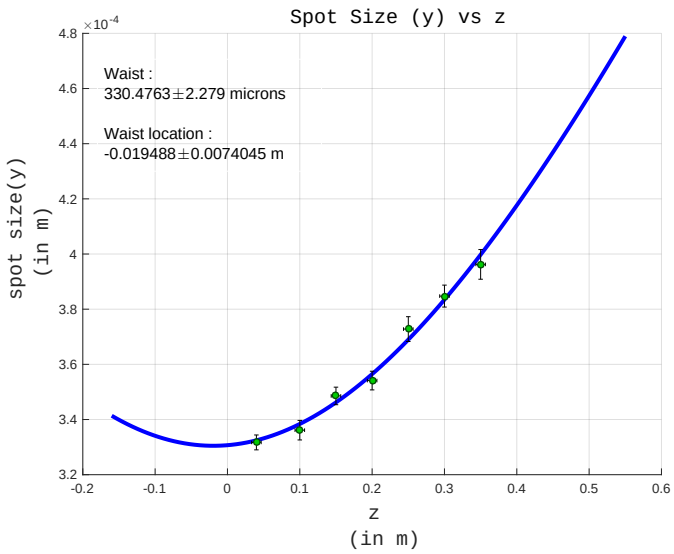

Figure 20: Beam Waist Size and Location

References

[1] LIGO Scientific Collaboration, *Advanced LIGO*. Class. Quant. Gravity 32, 074001 (2015)

[2] Buonanno, Alessandra and Chen, Yanbei, *Quantum noise in second generation, signal-recycled laser interferometric gravitational-wave detectors*

PhysRevD.64.042006

[3] LIGO Scientific Collaboration, *Instrument Science White Paper*. LIGO-T1600119v4 https://dcc.ligo.org/LIGO-T1600119/public

[4] LIGO Scientific Collaboration, *Enhanced sensitivity of the LIGO gravitational wave detector by using squeezed states of light* Nature Photonics 7, 613619 (2013)

[5] LIGO Scientific Collaboration, *A gravitational wave observatory operating beyond the quantum shot-noise limit* Nature Phys. 7, 962965 (2011)

[6] Alex Lvovsky, *Squeezed Light*. arXiv:1401.4118 .

[7] A. Ghatak and K. Thyagrajan , *Chapter 14, Optical Electronics*.

[8] Anthony Siegman, *Chapter 20, Lasers*.

[9] The Virgo Collaboration *Chapter 3, The VIRGO Physics Book Vol II - Optics and Related Topics*.

[10] M.S. Stefszky et al, *Balanced Homodyne Detection of Optical Quantum States at Audio-Band Frequencies and Below*.

[11] Hiro Yamamoto *Separation of adaptive scaling in the field propagation in x and y* LIGO-T1300995-v1